

Efficiently simulating personal vehicle energy consumption in mesoscopic transport models

Zachary A. Needell

Institute for Data, Systems, and Society
Department of Civil and Environmental Engineering
Massachusetts Institute of Technology
77 Massachusetts Avenue Cambridge, MA 02139
Email: zneedell@mit.edu

Jessika E. Trancik (Corresponding Author)

Institute for Data, Systems, and Society
Massachusetts Institute of Technology
77 Massachusetts Avenue Cambridge, MA 02139
Santa Fe Institute
Santa Fe, New Mexico 87501
Phone: 617-715-4552, Fax: 617-258-7733, Email: trancik@mit.edu

Word Count: 6,493 words + 2 figures + 2 tables = 7,493 words

Submission Date: November 15, 2017

1 ABSTRACT

2 Mesoscopic transport models can efficiently simulate complex travel behavior and traffic patterns
3 over large networks, but simulating energy consumption in these models is difficult with traditional
4 methods. Since mesoscopic transport models rely on a simplified handling of traffic flow, they can-
5 not provide the accurate second-by-second measurement of vehicle speeds and accelerations that
6 are required for widely-used energy models. Here we present extensions to the TripEnergy model
7 that fill in the gaps of low resolution trajectories with realistic contextual driving behavior. TripEn-
8 ergy also includes a vehicle energy model capable of simulating the impact of traffic conditions on
9 energy consumption and CO₂ emissions, with inputs in the form of widely-available calibration
10 data, allowing it to simulate thousands of different real-world vehicle makes and models. This
11 design allows TripEnergy to integrate with mesoscopic transport models and to be fast enough to
12 run on a large network with minimal additional computation time. We expect it to benefit from and
13 enable advances in transport simulation, including optimizing traffic network controls to minimize
14 energy, evaluating the performance of different vehicle technologies under wide-scale adoption,
15 and better understanding the energy and climate impacts of new infrastructure and policies.

1 INTRODUCTION

2 A variety of transport simulation models allow researchers and policymakers to predict the behav-
3 ior of travelers in great detail under different policy, infrastructure, and travel demand scenarios.
4 Producing energy-use and emissions estimates with these models opens up an even larger set of
5 possible research and policymaking applications—from estimating the emissions implications of
6 different policies or traffic control strategies to evaluating the expected usage patterns of emerging
7 vehicle technologies. However, barriers still remain to widespread application of linked transport
8 and energy/emissions models. In this paper, we present a new, flexible energy model calibrated on
9 a large sample of GPS driving behavior data and capable of linking with a mesoscopic transport
10 model to efficiently produce energy estimates for personal vehicles on large transport networks.

11 To be widely applicable to transport simulation, an energy model must balance efficiency
12 and specificity (*1*). Increases in computational power allow city-sized transport networks to be
13 simulated at the agent level—capturing the travel-related decisions and movements of millions of
14 travelers at a seconds time-scale. These models can simulate congestion, trip-making decisions,
15 and traveler response to information and incentives to a degree that is fundamentally impossible
16 with simpler models. The massive scale of these simulations require that any energy model op-
17 erating at vehicle scale operate very quickly and with minimal memory overhead. However, the
18 large number of different vehicle types on the road and the variety of operating conditions they
19 face during real-world use also require that any energy model either depend on vast amounts of
20 calibration data or incorporate major simplifications. While striking this balance, a useful model
21 must capture the relationship of vehicle energy use to the congestion, driver behavior, and external
22 conditions that motivate the use of complex transport models in the first place.

23 Here we present an extension of the existing TripEnergy model (*2*), allowing for the ef-
24 ficient linking of a mesoscopic transport simulation model with an energy model calibrated to
25 reproduce real-world energy use for a wide range of personal vehicles. By relying primarily on
26 empirical observations and simple physical approximations, this energy model uses fewer tunable
27 parameters than other methods. It neither requires high-resolution simulation of individual vehi-
28 cle motion, nor does it use traffic flow theory to fill in the gaps of the moderate-resolution vehicle
29 trajectories produced by more computationally efficient mesoscopic models. Both of these alterna-
30 tive approaches require calibration against disaggregate data that, while available for traffic counts
31 and speeds, are far more difficult to incorporate when the error to be minimized is against energy
32 consumption (*31*). Instead, the model presented here draws from a database of over 100,000 GPS
33 speed histories taken from various statewide travel surveys of real-world drivers (*2–5*) and fills
34 in the gaps of moderate-resolution simulated trajectories with representative examples of realistic
35 high resolution driving behavior. This energy model also does not require detailed emission rates
36 as inputs, instead using a simple vehicle energy model that can be calibrated on widely-available
37 regulatory data but that still reproduces energy consumption accurately enough for most purposes,
38 allowing thousands of individual vehicle types to be simulated with minimal additional calibration.
39 It achieves sufficient computational efficiency to run on large-scale networks through a novel sep-
40 aration of the driving behavior and vehicle performance steps of the energy estimation procedure.

41 This paper outlines the extensions to TripEnergy that allow it to process mesoscopic trans-
42 portation model outputs, describes a validation procedure for the matching method and energy
43 estimates, and presents results of simulation on a test network. We describe the energy estimation
44 procedure in two steps—a vehicle model that translates characteristics of a high-resolution trajec-
45 tory into an energy estimate, and a driving behavior model that links moderate-resolution simulated

1 vehicle trajectories to a database of high-resolution trajectories. Model validation is performed by
2 down-sampling drive cycles to moderate resolution and then application of the driving behavior
3 and vehicle models, comparing results to energy estimates given full knowledge of the trajectory
4 and a much more detailed vehicle simulation (6) and dynamometer results (7). The model is then
5 linked to the SimMobility mesoscopic transport simulation model (8) and results are examined for
6 a toy road network, reproducing expected energy performance for a range of different real-world
7 vehicle models.

8 **BACKGROUND**

9 **Traffic Network Modeling**

10 Transport models work by considering the relationship between transportation supply and demand.
11 The characteristics of the road and transit network such as travel times and costs are considered
12 in the supply model, while the demand model considers the destinations, departure times, modes,
13 and route choices for individuals' trips.

14 On the supply side, the state-of-the-art strategy is Dynamic Traffic Assignment (DTA),
15 which involves moving vehicles through the traffic network based on real-time traffic conditions
16 (9). Modern implementations of this method are able to capture certain effects, such as grid-
17 lock, queuing, and rerouting, that cannot be easily modeled using static methods. Some vehicle-
18 following models directly simulate acceleration, lane changing, and gap-acceptance behavior, and
19 given extensive calibration, could reproduce the realistic high-resolution vehicle trajectories nec-
20 essary to estimate energy use. However, it is often infeasible to run such detailed models on large
21 networks. As an alternative, mesoscopic models are able to capture many of the complex aspects of
22 transport supply while still achieving sufficient computational efficiency to run on large networks.
23 Mesoscopic models also follow individual agents across the network, but they contain a simplified
24 treatment of vehicle movement and often operate at a lower temporal resolution, typically on the
25 order of five to fifteen seconds. While sacrificing some details such as variability in driving style
26 and complex interactions between vehicles, such mesoscopic methods have been successfully ap-
27 plied to large networks (10) and can run quickly enough to optimize controls and interventions
28 (11). Mesoscopic traffic supply is included in many popular transport simulation models, such as
29 SimMobility Midterm (8), DTALite (12), and MATSIM (13).

30 On the demand side, most state-of-the-art models are "activity based." Unlike more tradi-
31 tional methods, activity based models simulate trip-making decisions in terms of how they allow
32 travelers to complete a daily sequence of activities. Activity based models can capture more real-
33 istic feedback between transportation network performance and travel demand, and they are better
34 suited to tracking individual travelers' location (and energy consumption) throughout the day (14).
35 Energy modeling is more closely related to the supply side of the modeling framework, as the
36 energy consumption of each vehicle depends on the details on its trajectory through the trans-
37 portation network. However, certain questions can be fully answered only by integrating energy
38 calculations directly into the supply/demand interaction. For example, the limited range of existing
39 battery-electric vehicles means that charging requirements will likely become a greater component
40 of travel decision-making, motivating development of energy models that can run in concert with
41 transport supply and demand calculations.

Model	Resolution Needed	Energy Method
COPERT-micro (15)	Link	Speed
EMFAC (16)	Trip	Speed
ADVISOR(6)	High-resolution	Microsimulation
VT-Micro (20)	High-resolution	Speed/Acceleration
EMEP/EEA (21)	High-resolution	VSP
MOVES County (22)	Link	VSP
MOVES Project (22)	High-resolution	VSP
MOVESlite (23)	High-resolution	VSP
VT-Macro (24)	Link	Speed/Acceleration
Zhou et al (25)	Mesosopic	VSP

TABLE 1 : Summary of selected methods to calculate energy based on transport network simulations.

1 Vehicle Modeling

2 Transport models of all sorts implicitly or explicitly simulate vehicle movement, and there exist
3 various software tools to turn simulated trajectories into energy estimates given a vehicle type.
4 These characterizations of vehicle movement can vary in terms of their temporal resolution and
5 the fidelity to which they can be expected to mimic real driving behavior, leading to different
6 scales at which energy models must operate.

7 Most traditional transport simulations model supply based on average speeds and densities
8 of links on the road network. These link-level speeds can be turned into energy estimates by models
9 such as COPERT (15) that rely on empirical measurements of typical energy and emissions rates
10 but do not directly capture the local effects of accelerations on energy use. Link speeds can also
11 be aggregated into beginning-to-end trip average speeds, which can be used to estimate energy
12 consumption by models such as EMFAC (16).

13 If a network simulation produces high-resolution trajectories (typically 1 Hertz or greater),
14 those trajectories can be fed into detailed vehicle simulations such as ADVISOR (6). These models
15 simulate the mechanics of vehicles in great detail and are best equipped to simulate complicated
16 processes such as criterion pollutant emissions or engine performance under extreme operating
17 conditions. However, these detailed models are slow to run, making them impractical to run on the
18 output of large network simulations.

19 To achieve greater efficiency while still capturing the detail provided by high-resolution tra-
20 jectories, researchers have developed simpler models to approximate vehicle performance. Some
21 estimate energy consumption rates based on polynomial fits to instantaneous speed (15) and others
22 use fits based on speed and acceleration, including the widely-used VT-Micro model (17). To bet-
23 ter incorporate factors such as road grade, a number of models estimate energy and emissions rates
24 using vehicle specific power (VSP), a measure of the relative power being used by the engine. One
25 commonly used VSP-based model is CMEM (18), which relies on measurements from a variety of
26 different vehicle types that cover the breadth of models in the on-road vehicle fleet. Other vehicle
27 models, some requiring less calibration data, have been proposed and evaluated as well (19).

28 One particularly comprehensive and widely-used energy and emissions model is MOVES
29 (22), which uses a database of emissions rates for a large number of different vehicle types over a

1 variety of speed and VSP bins known as operating modes. The distribution of time spent in each
2 of these operating mode bins for a geographic area is estimated based on a combination of disag-
3 gregate speed, temperature, travel behavior, and vehicle fleet data. MOVES can be cumbersome to
4 run at its most detailed settings, so for the added efficiency and flexibility others have developed
5 a simplified version, MOVESLite(23), with a more limited but still comprehensive set of vehicle
6 types and operating modes.

7 In all of these cases, there is an underlying difficulty: efficient simulation of large networks
8 requires some sort of simplification in the treatment of traffic flow, but energy consumption mod-
9 eling requires a high-resolution representation of vehicle movement. This tradeoff is apparent in
10 the various available levels of detail in MOVES. At the ‘County’ level, MOVES populates its op-
11 erating mode distribution table with results from a small set of high-resolution drive cycles, and
12 then calculates aggregate emissions by weighting these operating mode distributions for different
13 vehicle types based on traffic patterns. This method, however, is not capable of directly simulating
14 individual vehicle consumption or taking advantage of the full level of detail present in simulated
15 mesoscopic trajectories. At the higher-detail Project level, however, MOVES requires as inputs
16 drive schedules or operating mode distributions for each road link. To provide these inputs, it is
17 necessary either to run a full high-resolution simulation of the network or to rely on default val-
18 ues that do not reflect local traffic conditions. In practice, this means that there is no widely-used
19 energy estimation methodology that is capable of taking advantage of both the computational effi-
20 ciency of mesoscopic models as well as their ability to capture individual vehicle trajectories at a
21 higher resolution than link average speeds.

22 More recently, some researchers have proposed inferring detailed trajectory information
23 from the moderate-resolution trajectories produced by mesoscopic network simulations. This ap-
24 proach has been implemented (24, 25) using traffic flow theory to model the acceleration behavior
25 of drivers based on traffic density, and then inferring vehicle specific power from these interpo-
26 lated trajectories. The method we present has three main differences. First, TripEnergy fills in the
27 details of mesoscopic trajectories with empirical, real-world behavior, requiring fewer calibration
28 parameters; second, it is designed to simulate the energy consumption of a large number of real-
29 world vehicle types without needing large amounts of calibration data for each one; and third, it
30 uses a simpler model of instantaneous vehicle energy use, trading the ability to simulate emission
31 of non-CO₂ pollutants and engine performance under extreme operating conditions to allow for
32 more flexible and efficient implementation using a linear model.

33 **METHODS**

34 **Vehicle Model**

35 *Drive Energy*

36 This method of calculating energy consumption from a high-resolution trajectory relies on a sim-
37 plification that allows the important aspects of the trajectory to be stored in a vehicle-independent
38 manner but allows energy consumption for any vehicle type to be efficiently calculated from those
39 stored values. The basis for the energy model is the version presented in a previous paper (2) and
40 applied to questions of range constraints in battery electric vehicles (26), reformulated here to de-
41 pend only on instantaneous quantities. Unlike other pollutants such as CO and particulate matter,
42 CO₂ emissions from a gasoline-powered vehicle are almost precisely linearly related to the energy
43 content of the fuel used, allowing this method to be a useful way of estimating CO₂ emissions from
44 gasoline-powered vehicles as well.

1 The basis for the energy calculations is the tractive power, a function of the vehicle's instan-
 2 taneous speed v , acceleration a , and slope θ , as well as its mass m , a set of polynomial coastdown
 3 coefficients A , B , and C , and a rotational inertia fraction ε , set to be 0.05 here (27):

$$\mathcal{P}_{tr}(t) = Av(t) + Bv(t)^2 + Cv(t)^3 + (1 + \varepsilon)mv(t)a(t) + mg \sin(\theta(t))v(t) \quad (1)$$

4 In this paper, final energy quantities are written in script, whereas pre- conversion energy values
 5 (measured at the battery or gas tank) are written in normal font.

6 The rate of change of stored energy in the gas tank or in the battery consists of power going
 7 to the wheels, returning via the brakes (if regenerative braking exists), and going towards auxiliary
 8 electronics such as climate control. All of these processes involve conversion losses, taken into
 9 account with loss functions $P = L(\mathcal{P})$. The rate of change of energy stored in the vehicle is
 10 the power going towards motion $P_{accel} = L_{accel}(\mathcal{P}_{tr})$ minus the power sourced from regenerative
 11 brakes $P_{brake} = L_{brake}(\mathcal{P}_{tr})$, plus power going to the auxiliaries $P_{aux} = L_{aux}(\mathcal{P}_{aux})$, which depends
 12 on climate control and dashboard settings.

13 For clarity, we can define an indicator function for whether tractive power is positive (and
 14 the engine is active) or negative (and the brakes are active):

$$PTF(t) = \begin{cases} 1 & \mathcal{P}_{tr}(t) > 0 \\ 0 & \mathcal{P}_{tr}(t) \leq 0, \end{cases} \quad (2)$$

Finally, we make the further simplifying assumption that all of the loss functions are linear and that auxiliary power is constant over the course of a trip. The linear approximation has been shown to be reasonably accurate for internal combustion engine vehicles (28), and the framework we present here can easily be adjusted to allow for higher order polynomial terms, such as those tested by Saerens et al. (19). Using the linear approximation we have $L_{accel}(\mathcal{P}_{tr}(t)) = P_{idle} + \frac{\mathcal{P}_{tr}(t)PTF(t)}{\eta_{max}}$, $L_{brake}(\mathcal{P}_{tr}(t)) = \eta_{brake}\mathcal{P}_{tr}(t)(1 - PTF(t))$, and $L_{aux} = \frac{\mathcal{P}_{aux}}{\eta_{aux}}$. P_{idle} is the rate of energy use at no tractive power (including rest and coasting), in effect accounting for lower engine efficiency at low power. η_{max} is the slope of the \mathcal{P}_{tr} - P_{tr} line, in effect giving the engine efficiency approached at higher power. η_{brake} is the portion of energy going through the brakes re-cycled into the vehicle's battery and then back to the wheels. Defining the acceleration energy and braking energy as

$$\mathcal{E}_{accel} = \int_{t=0}^T \mathcal{P}_{tr}(t)PTF(t)dt; \quad \mathcal{E}_{brake} = \int_{t=0}^T -\mathcal{P}_{tr}(t)(1 - PTF(t))dt, \quad (3)$$

15 we can simplify the total energy equation:

$$E_{use} = \frac{\mathcal{E}_{accel}}{\eta_{max}} - \eta_{brake}\mathcal{E}_{brake} + \left(P_{idle} + \frac{\mathcal{P}_{aux}}{\eta_{aux}} \right) T. \quad (4)$$

16 This function for \mathcal{E}_{accel} is heavily dependent on the distance traveled and the average speed
 17 of the trip, so we can separate out the effects of these two quantities by replacing t , $v(t)$ and $a(t)$
 18 with unitless quantities: $\tau = (t - t_0)/T$, $u(\tau) = v(\tau)/\bar{v}$, and $\alpha(\tau) = a(\tau)/a_0$, where T is the total

1 duration of the drive cycle, \bar{v} is its average speed, and a_0 is a characteristic acceleration, defined
 2 here as 0.15 m/s^2 .

3 We can express the equation for \mathcal{E}_{accel} by defining a set of ‘moments’ consisting of the
 4 time-integrals of these unitless quantities:

$$\begin{aligned} \mu_1 &= \int_{\tau=0}^1 u(\tau)PTF(\tau)d\tau & \mu_2 &= \int_{\tau=0}^1 u(\tau)^2PTF(\tau)d\tau \\ \mu_3 &= \int_{\tau=0}^1 u(\tau)^3PTF(\tau)d\tau & \mu_a &= \int_{\tau=0}^1 \alpha(\tau)u(\tau)PTF(\tau)d\tau \end{aligned} \quad (5)$$

5 These definitions allow us to express the total acceleration energy without any integrals:

$$\mathcal{E}_{accel} = D(A\mu_1 + B\bar{v}\mu_2 + C\bar{v}^2\mu_3 + (1 + \varepsilon)m\alpha_0\mu_a + mg\Delta Z\mu_1) \quad (6)$$

6 where D is the total distance traveled. For the road grade component, and we assume that road
 7 grade is relatively constant over each time interval, leaving the energy impact dependent on the
 8 total elevation change ΔZ . Braking energy is calculated similarly for $PTF(t) < 0$, for which we
 9 define the comparable moments as v_i :

$$\mathcal{E}_{brake} = -D(Av_1 + B\bar{v}v_2 + C\bar{v}^2v_3 + (1 + \varepsilon)m\alpha_0v_a + mg\Delta Zv_1). \quad (7)$$

10 These two equations and an estimate of auxiliary power yield total energy consumption via Equa-
 11 tion 4. Pulling these average quantities outside of the integral in effect treats the total energy
 12 consumption as a linear combination of these average quantities multiplied by correction factors
 13 that depend on the specific details of the true speed history. The final expression for energy con-
 14 sumption is a linear combination of ten terms relating to the vehicle and its use:

$$\mathbf{V} = \begin{bmatrix} A/\eta_{max} \\ B/\eta_{max} \\ C/\eta_{max} \\ (1 + \varepsilon)m/\eta_{max} \\ A\eta_{brake} \\ B\eta_{brake} \\ C\eta_{brake} \\ (1 + \varepsilon)m\eta_{brake} \\ P_{idle} \\ 1/\eta_{aux} \end{bmatrix}; \quad \mathbf{U} = D \begin{bmatrix} 1 \\ \bar{v} \\ \bar{v}^2 \\ 1 \\ -1 \\ -\bar{v} \\ -\bar{v}^2 \\ -1 \\ 1/\bar{v} \\ \mathcal{P}_{aux}/\bar{v} \end{bmatrix} \circ \begin{bmatrix} \mu_1 \\ \mu_2 \\ \mu_3 \\ \alpha_0\mu_a \\ v_1 \\ v_2 \\ v_3 \\ \alpha_0v_a \\ 1 \\ 1 \end{bmatrix}; \quad E_{drive} = \sum_{k=1}^{10} V_k U_k. \quad (8)$$

15 These moments are a helpful way of expressing the total energy because they are almost
 16 independent of vehicle type. This is a simplification only because the function $PTF(t)$ varies
 17 slightly from vehicle to vehicle, but these differences end up having little effect on the total energy

1 and are ignored here. The moments, calculated for a partial or full vehicle trajectory, can serve a
 2 similar purpose to the link-specific driving schedules or operating mode distributions required as
 3 an input to MOVES, defining the factors of a vehicle’s use that determine energy requirements.
 4 Rather than querying a detailed set of vehicle-specific emissions rates or evaluating integrals, all
 5 that is needed to evaluate this energy function is to access these stored parameters that can be
 6 calculated in advance, allowing for faster computation.

7 *Drive Efficiency Calibration*

The vehicle-specific component of the total energy in Equation 8, \mathbf{V} , depends in part on physical vehicle road load characteristics A , B , C , m that are all published by the US EPA (29). The remaining three parameters, P_{idle} , η_{max} , and η_{brake} are estimated by approximating measured energy consumption over a set of EPA test cycle results, similar to methods proposed elsewhere (2, 19, 26, 30). We minimize mean squared error between the predicted (MPG_{est}) and measured (MPG) fuel economy values for a set of test cycles DC with known fuel economy:

$$\underset{P_{idle}, \eta_{max}, \eta_{brake}}{\operatorname{argmin}} \sum_{i \in DC} (MPG_i - MPG_{est_i}(P_{idle}, \eta_{max}, \eta_{brake}))^2. \quad (9)$$

8 For light duty vehicles, these drive cycles can consist of the EPA city (FTP) and highway (HWFET)
 9 drive cycles, as well as for the high speed (US06) cycle for the vehicles with it available. For this
 10 paper, we calibrate these parameters for 3,784 vehicle types with model years from 2010 to 2016.
 11 During calibration, P_{brake} is fixed to 0 for vehicles without regenerative braking. For vehicles with
 12 regenerative braking but only two test cycles available, P_{idle} is fixed—to 1409 W for hybrid electric
 13 vehicles and 741 W for fully electric vehicles—to ensure a unique solution. The value for hybrid
 14 electric vehicles is chosen by taking the median fit value for P_{idle} of the hybrid vehicles for which
 15 three unique fuel economy estimates are available. The value for fully electric vehicles is fixed
 16 to the value for P_{idle} found by calibrating the 2013 Nissan Leaf on additional drive cycles whose
 17 energy consumption is provided in the Downloadable Dynamometer Database (7).

18 Each vehicle being simulated in the transport model linked to TripEnergy must be assigned
 19 a specific vehicle type and associated energy parameters. Accurately assigning each simulated
 20 agent with a correct vehicle type is likely too burdensome to be worthwhile for many applications,
 21 and in such cases a representative vehicle can be chosen for different vehicle categories available
 22 to the population. For cases where more detail in the vehicle fleet is required, vehicle types can
 23 be assigned to households by a discrete choice model as part of the population synthesis. This
 24 functionality is especially useful for emerging integrated models where household location and
 25 vehicle ownership decisions are tied to the utilities of different transportation alternatives (8).

26 **Drive Cycle Matching**

27 We frame the process of estimating energy consumption from simulated trajectories as a prediction
 28 problem. Given limited information about a vehicle j ’s characteristics: \mathcal{V}_j , and about its trajectory:
 29 \mathcal{U}_j , we estimate the expected value of a vehicle’s energy consumption over timestep i under those
 30 conditions: $E[E_{ij} | \mathcal{U}_j, \mathcal{V}_j]$. In this case, the information known is the vehicle’s cumulative distance
 31 traveled every advance interval, and vehicle characteristics. We assume that the vehicle could have
 32 followed any speed profile over each timestep, but that the measurements at advance intervals are
 33 accurate. The linear nature of Equation 8 means that the goal becomes to predict the components
 34 of the moment vector \mathbf{U} for each timestep given the vehicle’s trajectory \mathcal{U} :

$$E[E_{ij}|\mathcal{U}_j, \mathcal{V}_j] = E \left[\left(\sum_{k=1}^{10} U_{ijk} V_{jk} \right) | \mathcal{U}_j, \mathcal{V}_j \right] = \sum_{k=1}^{10} E[U_{ijk}|\mathcal{U}_j] V_{jk}. \quad (10)$$

1 We estimate $E[\mathbf{U}_{ij}|\mathcal{U}_j]$ by searching a database of real-world drive cycles for intervals that are sim-
 2 ilar to the portion in advance interval i being estimated. The vector of moments can be calculated
 3 for each matched trajectory segment and then averaged, producing an estimate $\bar{\mathbf{U}}_{ij}$ of those mo-
 4 ments for the unknown partial trajectory, which can then be combined with the vehicle parameters
 5 \mathbf{V}_j to estimate E_{ij} .

6 This matching and averaging procedure has several advantages. It can be implemented
 7 efficiently, it does not require that detailed energy use measurements be stored for multiple vehicle
 8 types, and it is robust to modeling decisions about driving style that must be made for short-term
 9 simulations—a useful property because trajectories simulated by short-term models might not be
 10 entirely accurate or consistent for energy-consumption purposes (31). This solution for storing
 11 driving moments does not directly incorporate elevation change. For networks where elevation
 12 change is expected to greatly effect energy consumption, separate moment databases can be created
 13 for different grades and accessed based on the instantaneous grade of the simulated vehicle at each
 14 timestep.

15 To efficiently implement this matching procedure, we create a lookup table of averaged
 16 moments that can be accessed based on binned properties of the medium-resolution trajectory.
 17 For instance, the lookup table for a simple speed-based matching scheme can be implemented
 18 by breaking each GPS drive-cycle into segments of the same duration as the advance interval,
 19 assigning each segment to a bin based on its average speed, calculating the mean moments for
 20 each bin, and then using those mean moments to calculate $E[\mathbf{U}_{ij}|\mathcal{U}_j]$. The drive cycle database
 21 used for matching consists of over 100,000 trips with 1-Hz speed measurements and has been
 22 described in detail (2–5).

23 Various matching methods are possible. A one-dimensional matching scheme (\bar{v}_t) was
 24 tested, using only the average speed over the current advance interval. This is expected to give
 25 results similar to a best-possible method based only on timestep average speed, assuming the driv-
 26 ing behavior in the area being modeled is relatively similar to that captured in the driving behavior
 27 database. Two two-dimensional schemes were tested: one based on the current and previous av-
 28 erage speeds (\bar{v}_{t-1}, \bar{v}_t) and one based on the average speed and average acceleration of the current
 29 advance interval (\bar{v}_t, \bar{a}_t), with average acceleration determined based on the instantaneous speeds
 30 at the beginning and end of the advance interval¹. Two three-dimensional matching schemes were
 31 tested: one based on the average speed over the current advance interval as well as the instanta-
 32 neous speeds its the beginning and end (\bar{v}_t, v_i, v_f), and one based on the average speed over the
 33 preceding, current, and following advance intervals ($\bar{v}_{t-1}, \bar{v}_t, \bar{v}_{t+1}$).

34 As explained below, the most accurate was found to be matching based on a trajectory’s
 35 average speed over a given advance interval, the previous interval, and following interval. Here, we
 36 divide speeds into 38 bins in each of three dimensions, leading to 54,872 individual bins, each of
 37 which needs to store 8 different moments—a data structure that can be accessed quickly and uses
 38 a non-substantial amount of memory. This database is sufficiently well populated if it captures the
 39 extent of movements experienced during typical driving well enough to provide a valid expected

¹Accurate instantaneous speeds is a possible output of some but not necessarily all mesoscopic traffic simulations

1 value for the moments in each bin. A large set of drive cycles is needed to populate this database,
2 and additional drive cycles can be added as needed. Indeed, 84.5% of the bins for which there are
3 at least 10 observations in the GPS dataset are not observed at all in the 49 drive schedules provided
4 in the MOVES database. These behaviors not observed in the MOVES database account for 29%
5 of the total driving time in the GPS dataset, showing the value of incorporating this additional
6 driving behavior.

7 A visualization this lookup table is shown in Figure 1. The average speed over the advance
8 interval being estimated is fixed for each of the three columns, the average speed for the previous
9 time interval determines the y-position and the average speed for the next time interval determines
10 the x-position within each subfigure². The first row of subfigures shows the number of observations
11 in each bin, with much of the range of plausible vehicle movements having over 1,000 distinct 5-
12 second observations. The second row shows the average value of μ_1 , a moment relating to the
13 portion of time during which the engine was active. The third row shows the average value of μ_a ,
14 a moment related to the amount of work the engine does towards acceleration.

²For example, the pixel at $Y = 35$, $X = 45$ in the middle (41 mph) column of Figure 1 represents drive cycle segments averaging 41 mph and accelerating—where the previous interval averaged 35 mph and the following interval will average 45 mph.

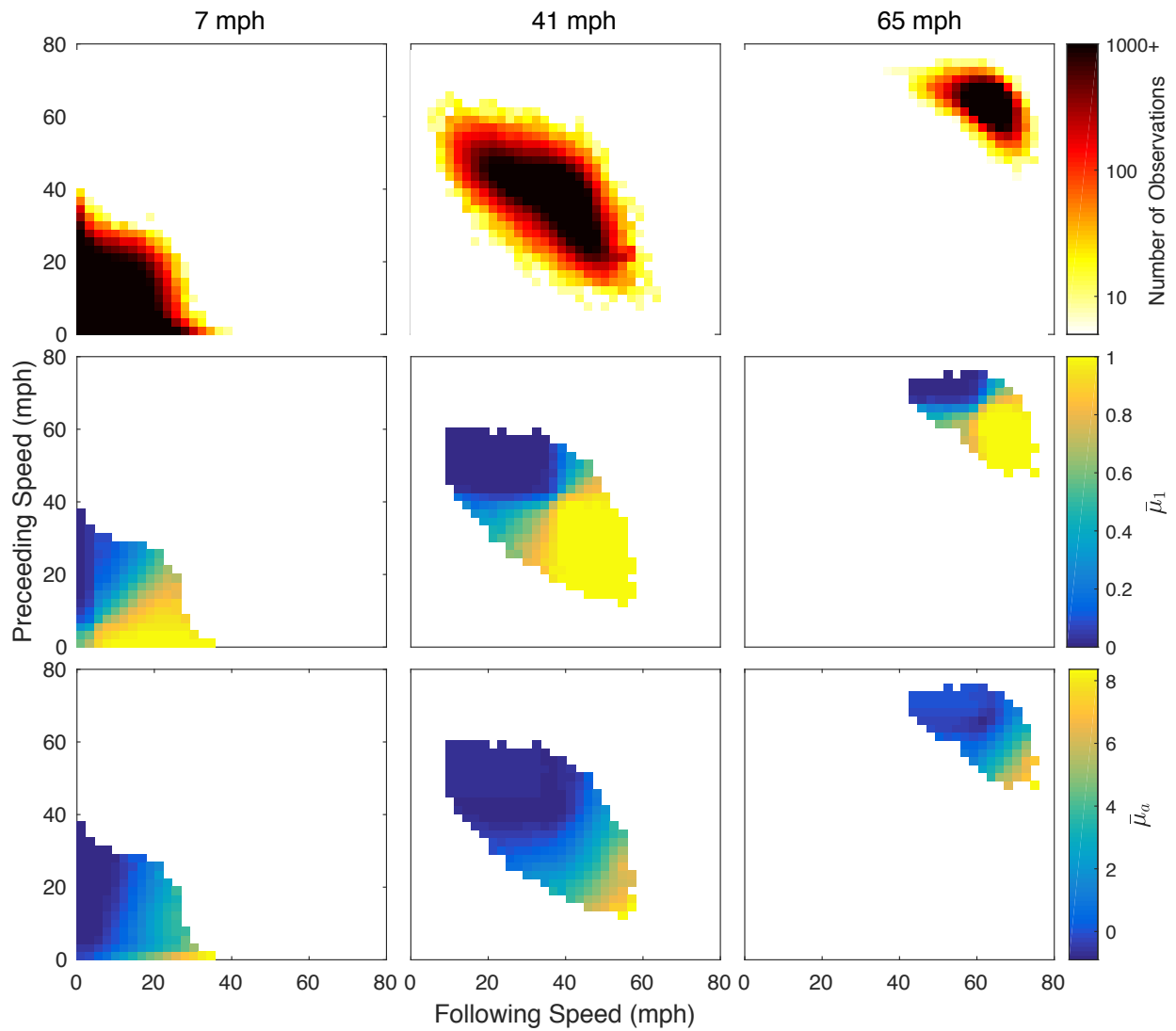


FIGURE 1 : Visualization of the lookup table of drive cycle moments produced by matching on three consecutive average speeds, for a 5-second advance interval.

1 MODEL VALIDATION

2 Microsimulation

3 The preferred matching methods was chosen based on the root mean square error of fuel economy
 4 predictions, ease of applicability to mesoscopic simulations, and robustness to errors in mesoscopic
 5 trajectories. Errors were calculated by comparing estimated energy values to ‘ground truth’ values
 6 given by microsimulation. 20% of approximately 100,000 available 1-hz GPS trajectories were
 7 chosen as a test set. These were converted into simulated mesoscopic trajectories by downsam-
 8 pling them into 5-second resolution average speeds, consistent with a mesoscopic simulation with
 9 a 5-second advance interval. An estimate for the true energy consumption was produced by simu-
 10 lating vehicle performance with the ADVISOR software (6). The vehicle simulated was a compact
 11 ICEV, with physical characteristics modeled after a 2014 Ford Focus. The vehicle model described
 12 above was then calibrated based on ADVISOR outputs—coastdown coefficients A , B , and C were
 13 estimated based on a polynomial fit to instantaneous road load, and drive cycle fuel economy mea-
 14 surements used for model calibration were produced by running the simulated vehicle through
 15 the EPA HWFET (Highway) and USDDS (City) drive cycles. The final vehicle model parame-
 16 ters used were $A : 172.8 N$, $B : -4.676 Ns/m$, $C : 0.5516 Ns^2/m^2$, $m : 1406 kg$, $P_{idle} : 11.50 kW$,
 17 $\eta_{max} : 0.4081$. No additional auxiliary energy use is assumed.

18 The remaining 80% of trips were used to generate a database of binned driving behavior
 19 moments as described above, using different binning methods. The robustness of the matching
 20 methods to errors in mesoscopic trajectories is tested by adding different degrees of uncorrelated
 21 random noise to individual timesteps in the medium-resolution trajectories.

Estimation Method	No noise		$\pm 1 mph$ noise		$\pm 2 mph$ noise	
	RMS (mpg)	Total	RMS (mpg)	Total	RMS (mpg)	Total
Spline	1.08	-2.2%	0.96	-1.2%	1.13	1.98%
\bar{v}_t	2.47	-0.78%	2.47	-0.73%	2.46	-0.55%
\bar{v}_{t-1}, \bar{v}_t	1.33	-0.65%	1.44	-0.19%	1.92	2.19%
\bar{v}_t, \bar{a}_t	0.93	-0.36%	1.08	0.50%	1.64	3.4%
\bar{v}_t, v_i, v_f	0.88	-0.40%	1.33	1.01%	2.39	4.12%
$\bar{v}_{t-1}, \bar{v}_t, \bar{v}_{t+1}$	0.90	-0.45%	0.99	-0.06%	1.47	2.24%
Vehicle Model	0.71	-0.28%	na	na	na	na

TABLE 2 : Performance of different matching methods given different levels of error in vehicle trajectories.

22 Models were compared based on root mean square estimation error for trip average fuel
 23 economy, given a five second advance interval. Two other models were simulated as a comparison,
 24 neither of which is expected to be as scalable to large-scale simulations. The ‘‘Spline’’ model in-
 25 terpolated the mesoscopic trajectory to a high-resolution one using cubic splines. ‘‘Vehicle Model’’
 26 assumes access to the true high-resolution trajectory, useful as a bound on the error introduced by
 27 the matching algorithm as opposed to the vehicle model.

28 Given accurate mesoscopic trajectories, the methods (\bar{v}_t, \bar{a}_t) , (\bar{v}_t, v_i, v_f) , and $(\bar{v}_{t-1}, \bar{v}_t, \bar{v}_{t+1})$
 29 all perform roughly equivalently, with root mean square errors of trip-averaged fuel economy of
 30 approximately 0.9 mpg, compared to RMS error of 0.71 mpg given high-resolution knowledge of
 31 the trajectory and 1.08 for the spline method, and an error for the estimated total energy of all trips

1 within 0.5% of the true value. Under increased uncertainty, the method based on three consecutive
2 average speeds outperforms those incorporating instantaneous measurements. At high uncertainty,
3 a spline-based method outperforms the methods based on binned moments, but all other binned
4 methods outperform the method (\bar{v}_t) based on only average speeds. Given these results, the three
5 dimensional ($\bar{v}_{t-1}, \bar{v}_t, \bar{v}_{t+1}$) method is chosen.

6 **Aggregate Performance Measures**

7 Additional evaluation was performed by running a simulation of a traffic network containing a
8 variety of vehicle types, comparing fuel economy measurements for the different vehicles to EPA
9 estimates. The transport network simulation was performed using SimMobility Midterm (8), a sim-
10 ulator linking an activity-based demand simulator with a mesoscopic, DTA supply model. TripEn-
11 ergy was implemented in C++ and run concurrently with SimMobility, leading to an increase in
12 simulation time and memory use of less than 5%. The tests were performed on the ‘Virtual City’
13 network, containing 94 nodes and 254 links, with constant elevation. The simulation was run for
14 a full day, during which vehicles made a total of 174,594 individual trips. Four vehicle types were
15 simulated—a 2013 Nissan Leaf (a battery-electric sedan), a 2016 Toyota Prius (a hybrid-electric
16 sedan), a 2014 Honda Accord plug-in hybrid operating in charge depleting mode (a sedan), and
17 a 2010 Ford F150 (a pickup truck). Additional auxiliary energy consumption of 1000 W was as-
18 sumed to account for typical auxiliary use. Charging efficiency of 83.7% was assumed for the Leaf
19 (32).

20 Vehicle fuel economies were then compared to EPA adjusted fuel economy estimates. Each
21 trip was classified as “Highway” (more than 50% of the time spent at greater than 55 mph), or
22 “City” for the remaining trips. Expected results were observed, with the gasoline internal com-
23 bustion engine-powered F150 achieving lower fuel economy for city driving, while the hybrid-
24 electric Prius and fully-electric Leaf typically achieving lower fuel economy for highway trips.

25 Average fuel consumption values for each vehicle over each class of trip were compared
26 to EPA-published “City” and “Highway” ratings, showing generally close agreement. EPA ad-
27 justed city/highway fuel economies for the Leaf, Prius, Accord PHEV in charge-sustaining mode,
28 F150 are 126/101, 58/53, 49/45, and 15/21, respectively. In this simulation, average stop-and-
29 go/highway fuel economies for the different vehicle types are 143/125, 59/55, 56/53, and 17/18,
30 respectively. EPA unadjusted fuel economy ratings are used in the calibration of the efficiency pa-
31 rameters in the TripEnergy vehicle model, but EPA adjusted values (typically lower) are produced
32 through a complicated process not factored into the TripEnergy model (33). Any agreement be-
33 tween TripEnergy results and EPA-adjusted values are the result of the less-energy-efficient driving
34 and additional auxiliary use present in SimMobility and the real world but not the unadjusted EPA
35 tests.

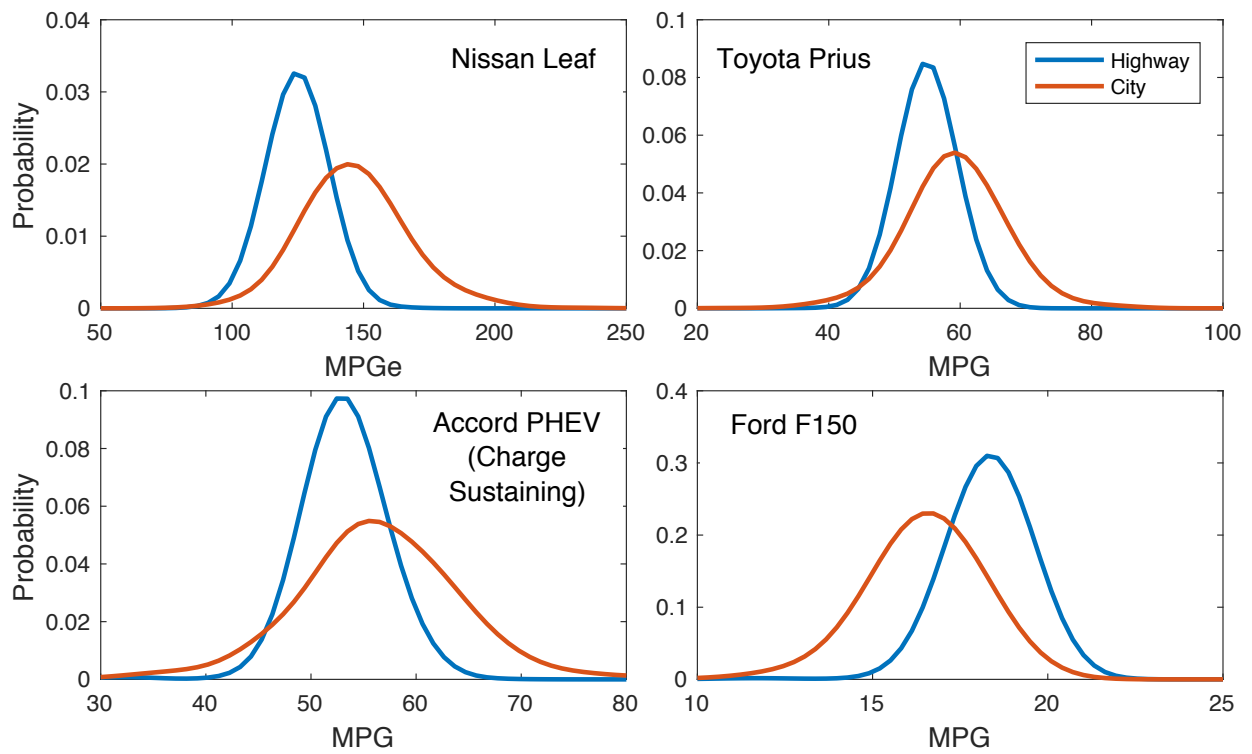


FIGURE 2 : Distribution of trip-averaged fuel economies for different vehicle types, simulated with SimMobility over the “Virtual City” road network.

1 **DISCUSSION**

2 This paper links an existing mesoscopic transport simulation with an energy model that can es-
3 timate the energy consumption and CO₂ emissions from personal vehicles. Given moderate res-
4 olution vehicle trajectories from a mesoscopic traffic model, TripEnergy can efficiently estimate
5 energy consumption more accurately than simple speed and acceleration-based methods. TripEn-
6 ergy offers various improvements more over widely-used methods such as MOVES: it utilizes the
7 full detail on vehicle movements provided by mesoscopic simulations; it is computationally ef-
8 ficient enough to be run concurrently with a transport model; and it produces energy estimates
9 that can be traced back to individual vehicles and agents. In addition, because it relies primarily
10 on independent measurements of high-resolution driving behavior, this method is less reliant than
11 alternative models on tunable parameters governing vehicle movement, which are not typically
12 calibrated to reproduce trajectories that are accurate from an energy perspective.

13 Because this model was developed to take advantage of the strengths of state-of-the-art
14 transport simulations, we expect it to prove increasingly useful as simulations continue to evolve
15 and be applied to new questions and research directions. These include problems where energy
16 consumption of vehicles needs to be integrated into agents' travel choice framework; where the
17 vehicles being studied do not have detailed energy-use measurements beyond EPA mandated tests;
18 and where energy consumption and CO₂ emissions, rather than other pollutants, are the primary
19 target of study. Such problems include the development of tools and policies targeted at individual
20 travelers, understanding the effects of fuel economy on long-term vehicle purchasing decisions,
21 and for studies of electric vehicle range and charging behavior. Additionally, the ability to calcu-
22 late energy consumption from limited-resolution trajectories will be useful for contexts outside of
23 traditional transport modeling, including suggesting energy-efficient routes given estimates of the
24 congestion state of a traffic network, or estimating energy consumption of a trip given trajectory
25 information captured by a smartphone.

26 In future work, several extensions to this analysis will be pursued. Further work is needed
27 to quantify the degree to which mesoscopic models capture realistic traffic movement. The im-
28 pacts of user-specific driving style on energy use and the degree to which the database of driving
29 behavior data captures this variability will also be investigated further. Finally, the vehicle model
30 could be augmented through the inclusion of additional, higher-order moments. The additional
31 energy estimation accuracy allowed by this modification will be assessed using onboard diagnostic
32 recorders in on-road vehicles, and the gains in accuracy will be weighed against the complexity
33 added to the vehicle model.

34 **ACKNOWLEDGEMENTS**

35 This work was supported by the New England University Transportation Center at MIT, the MIT
36 Leading Technology and Policy Initiative, the Singapore-MIT Alliance for Research and Technol-
37 ogy, the Charles E. Reed Faculty Initiatives Fund, and the MIT Energy Initiative. The information,
38 data, or work presented herein was funded in part by the Advanced Research Projects Agency-
39 Energy (ARPA-E), U.S. Department of Energy, under the TRANSNET program.

1 **REFERENCES**

- 2 [1] Casas, J., J. Perarnau, and A. Torday, The need to combine different traffic modelling levels
3 for effectively tackling large-scale projects adding a hybrid meso/micro approach. *Procedia-*
4 *Social and Behavioral Sciences*, Vol. 20, 2011, pp. 251–262.
- 5 [2] McNerney, J., Z. A. Needell, M. T. Chang, M. Miotti, and J. E. Trancik, TripEnergy: Esti-
6 mating POV energy consumption given limited travel survey data. *Transportation Research*
7 *Record: Journal of the Transportation Research Board (In Press)*, 2017.
- 8 [3] DOE National Renewable Energy Laboratory, *California Household Transportation Survey*.
9 DOE-019-9889603959, 2012.
- 10 [4] Atlanta Regional Commission, *Regional Travel Survey: Final Report*, 2011.
- 11 [5] Texas Department of Transportation, *2002 - 2011 Regional Travel Surveys with GPS data for*
12 *Abilene, Austin, El Paso, Houston Galveston, Laredo, Rio Grande Valley, San Antonio, Tyler*
13 *Longview, and Wichita Falls*, 2002-2011.
- 14 [6] Markel, T., A. Brooker, T. Hendricks, V. Johnson, K. Kelly, B. Kramer, M. O’Keefe, S. Sprik,
15 and K. Wipke, ADVISOR: a systems analysis tool for advanced vehicle modeling. *J Power*
16 *Sources*, Vol. 110, No. 2, 2002, pp. 255–266.
- 17 [7] Advanced Powertrain Research Facility (APRF), *Downloadable Dynamometer Database*.
18 Argonne National Laboratory (ANL), 2011.
- 19 [8] Adnan, M., F. C. Pereira, C. M. L. Azevedo, K. Basak, M. Lovric, S. Raveau, Y. Zhu, J. Fer-
20 reira, C. Zegras, and M. Ben-Akiva, SimMobility: A Multi-scale Integrated Agent-based
21 Simulation Platform. In *95th Annual Meeting of the Transportation Research Board Forth-*
22 *coming in Transportation Research Record*, 2016.
- 23 [9] Chiu, Y.-C., J. Bottom, M. Mahut, A. Paz, R. Balakrishna, T. Waller, and J. Hicks, Dynamic
24 traffic assignment: A primer. *Transportation Research E-Circular*, , No. E-C153, 2011.
- 25 [10] De Palma, A. and F. Marchal, Real cases applications of the fully dynamic METROPOLIS
26 tool-box: an advocacy for large-scale mesoscopic transportation systems. *Networks and spa-*
27 *tial economics*, Vol. 2, No. 4, 2002, pp. 347–369.
- 28 [11] Ben-Akiva, M. E., S. Gao, Z. Wei, and Y. Wen, A dynamic traffic assignment model for
29 highly congested urban networks. *Transportation Research Part C: Emerging Technologies*,
30 Vol. 24, 2012, pp. 62 – 82.
- 31 [12] Zhou, X. and J. Taylor, DTALite: A queue-based mesoscopic traffic simulator for fast model
32 evaluation and calibration. *Cogent Engineering*, Vol. 1, No. 1, 2014, p. 961345.
- 33 [13] Charypar, D., K. W. Axhausen, and K. Nagel, *An event-driven queue-based microsimula-*
34 *tion of traffic flow*. ETH, Eidgenossische Technische Hochschule Zurich, IVT, Institut fur
35 Verkehrsplanung und Transportsysteme, 2006.
- 36 [14] Bowman, J. L. and M. E. Ben-Akiva, Activity-based disaggregate travel demand model sys-
37 tem with activity schedules. *Transportation Research Part A: Policy and Practice*, Vol. 35,
38 No. 1, 2001, pp. 1–28.
- 39 [15] Samaras, C., L. Ntziachristos, and Z. Samaras, COPERT Micro: a tool to calculate the vehicle
40 emissions in urban areas. In *Transport Research Arena (TRA) 5th Conference: Transport*
41 *Solutions from Research to Deployment*, 2014.
- 42 [16] California Air Resource Board, *2.30 User guide: calculating emission inventories for vehi-*
43 *cles in California*, 2006.

- 1 [17] Rakha, H., K. Ahn, and A. Trani, Development of VT-Micro model for estimating hot stabi-
2 lized light duty vehicle and truck emissions. *Transportation Research Part D: Transport and*
3 *Environment*, Vol. 9, No. 1, 2004, pp. 49–74.
- 4 [18] Scora, G. and M. Barth, Comprehensive modal emissions model (cmem), version 3.01. *User*
5 *guide*. Centre for Environmental Research and Technology. University of California, River-
6 side, 2006.
- 7 [19] Saerens, B., H. Rakha, K. Ahn, and E. Van Den Bulck, Assessment of alternative polynomial
8 fuel consumption models for use in intelligent transportation systems applications. *Journal*
9 *of Intelligent Transportation Systems*, Vol. 17, No. 4, 2013, pp. 294–303.
- 10 [20] Ahn, K. and H. Rakha, The effects of route choice decisions on vehicle energy consumption
11 and emissions. *Transportation Research Part D: Transport and Environment*, Vol. 13, No. 3,
12 2008, pp. 151 – 167.
- 13 [21] Fontes, T., A. Lemos, P. Fernandes, S. Pereira, J. Bandeira, and M. Coelho, Emissions impact
14 of road traffic incidents using Advanced Traveller Information Systems in a regional scale.
15 *Transportation Research Procedia*, Vol. 3, 2014, pp. 41–50.
- 16 [22] Assessment and Standards Division, Office of Transportation and Air Quality, *Population*
17 *and Activity of On-road Vehicles in MOVES2014*. Draft Report EPA-420-D-15-001, U.S.
18 Environmental Protection Agency, 2015.
- 19 [23] Frey, H. C. and B. Liu, Development and evaluation of simplified version of MOVES for cou-
20 pling with traffic simulation model. In *Transportation Research Board 92nd Annual Meeting*,
21 2013, 13-1201.
- 22 [24] Zegeye, S., B. De Schutter, J. Hellendoorn, E. Breunese, and A. Hegyi, Integrated macro-
23 scopic traffic flow, emission, and fuel consumption model for control purposes. *Transporta-*
24 *tion Research Part C: Emerging Technologies*, Vol. 31, 2013, pp. 158–171.
- 25 [25] Zhou, X., S. Tanvir, H. Lei, J. Taylor, B. Liu, N. M. Rouphail, and H. C. Frey, Integrating a
26 simplified emission estimation model and mesoscopic dynamic traffic simulator to efficiently
27 evaluate emission impacts of traffic management strategies. *Transportation Research Part D:*
28 *Transport and Environment*, Vol. 37, 2015, pp. 123–136.
- 29 [26] Needell, Z. A., J. McNERney, M. T. Chang, and J. E. Trancik, Potential for widespread elec-
30 trification of personal vehicle travel in the United States. *Nature Energy*, Vol. 1, 2016, p.
31 16112.
- 32 [27] Larminie, J. and J. Lowry, *Electric Vehicle Technology Explained*. John Wiley & Sons, 2004.
- 33 [28] Post, K., J. Kent, J. Tomlin, and N. Carruthers, Fuel consumption and emission modelling
34 by power demand and a comparison with other models. *Transportation Research Part A:*
35 *General*, Vol. 18, No. 3, 1984, pp. 191–213.
- 36 [29] United States Environmental Protection Agency, *Certified Vehicle Test Results Report Data*.
37 Available <http://www.epa.gov/otaq/crttst.htm>, 2015.
- 38 [30] Lutsey, N., A technical analysis of model year 2011 US automobile efficiency. *Transp Res D*
39 *Transp Environ*, Vol. 17, No. 5, 2012, pp. 361–369.
- 40 [31] da Rocha, T. V., L. Leclercq, M. Montanino, C. Parzani, V. Punzo, B. Ciuffo, and D. Villegas,
41 Does traffic-related calibration of car-following models provide accurate estimations of vehi-
42 cle emissions? *Transportation research part D: Transport and Environment*, Vol. 34, 2015,
43 pp. 267–280.

- 1 [32] Forward, E., K. Glitman, and D. Roberts, *An assessment of level 1 and level 2 electric ve-*
2 *hicle charging efficiency*. Vermont Energy Investment Corporation Transportation Efficiency
3 Group, 2013.
- 4 [33] *Fuel Economy Labeling of Motor Vehicle Revisions to Improve Calculation of Fuel Economy*
5 *Estimates*. Office of Transportation and Air Quality, US EPA, 2006.